Available online at www.sciencedirect.com
SCIENCE DIRECT
Journal of Colloid and Interface Science 279 (2004) 192–197
JOURNAL OF Colloid and Interface Science
www.elsevier.com/locate/jcis

Capturing drops with a thin fiber

Élise Lorenceau [a], Christophe Clanet [b], David Quéré [a,*]

[a] *Laboratoire de Physique de la Matière Condensée, UMR 7125 du CNRS, Collège de France, 75231 Paris Cedex 05, France*
[b] *Institut de Recherche sur les Phénomènes Hors Équilibre, UMR 6594 du CNRS, BP 146, 13384 Marseille Cedex, France*

Received 4 December 2003; accepted 17 June 2004
Available online 24 July 2004

Abstract

We study experimentally the dynamics of drops impacting horizontal fibers and characterize the ability of these objects to capture the drops. We first show that a drop larger than a critical radius cannot be trapped by a fiber whatever its velocity. We determine this critical size as a function of the fiber radius. Then we show that for smaller drops, different situations can occur: at a low impact velocity, the drop is entirely captured by the fiber, whereas some liquid is ejected when arriving faster. We quantify the threshold velocity of capture.

Keywords: Impact; Wetting; Filtration

1. Introduction

Making fogs pass through filters (which consist of 3D networks of fibers) is a usual way to recover the liquid phase from an aerosol: the droplets are collected by the solid part of the grid while the gaseous phase pass through it. Such grids or filters are used to recover liquid from morning fog in a deserted area or to reduce the noxious emission of aerosol from chemical plants. It is of obvious practical interest to improve the efficiency of these filters. One difficulty may reside in the fact that this efficiency is strongly time-dependent: during the filtration process, the amount of liquid trapped in the filter bed increases and eventually clogs it. Recently, Contal et al. showed that clogging of fiber filters by liquid droplets can be described in four phases [1]. First, the droplets impact the wet fibers; then the amount of those droplets stuck on the fiber increases so that proximal droplets coalesce. In a third stage, the amount of collected liquid is large enough to form liquid shells in the net. This leads to a large increase of the pressure drop and to a dramatic decrease in the efficiency of the filter. Eventually, a pseudo-stationary state can be established between the droplet collection and the gravitational drainage of the liquid phase.

Several studies have been devoted to the early stage of the clogging of the filter, i.e., the stage of maximum efficiency. Patel et al. [2] studied the drop breakup in a flow through fiber filters and evaluated the breakup probability for a drop. Hung and Yao [3] also considered experimentally the impact of water droplets on a cylindrical object. Both these studies show that depending on the speed of the impacting droplets, the drops can be captured and break up into several pieces. In this article, we also focus on the first stage of the filtering and stress more precisely the impaction phenomena by considering a single droplet falling on a horizontal fiber. A filter consists mainly of three elementary patterns: fibers, holes, and small knots. Our analysis might thus complement those carried out in [4,5], in which the impact of a single drop on a small disk and a small hole was studied. We first demonstrate that even if gently deposited on a fiber, a drop can detach if the capillary force is not large enough to overcome its weight. The position of a drop dangling down a fiber is determined, from which we deduce the size of the largest hanging drop. Then we focus on the impact of a drop (smaller than this largest size) falling on a horizontal fiber and determine

* Corresponding author. Fax: +33-144271082.
E-mail address: david.quere@college-de-france.fr (D. Quéré).

0021-9797/$ – see front matter
doi:10.1016/j.jcis.2004.06.054

the threshold in velocity below which the drop is entirely captured.

2. Statics

2.1. Observations

We first focus on drops hanging from a horizontal fiber (made of copper) of radius b. A given volume Ω of silicon oil (controlled by using microsyringes) is gently deposited on a metallic fiber, which it wets completely.

Fig. 1 shows drops of silicon oil of increasing volume hanging at rest from a fiber of radius $b = 12$ μm. It can be seen that the shape of the drop changes as its volume increases: the two smallest drops are axisymmetric, but the largest drops are asymmetric. Carroll and McHale analyzed the different shapes of a drop on a fiber in the absence of gravity [6–8]. They found that the drop can adopt either an axisymmetric configuration (barrel shape) or an asymmetric one (clamshell shape). They pointed out that the barrel shape is favored when increasing the fiber wettability, and making the drop larger. In Fig. 1, the liquid totally wets the fiber and the volume of the drop increases as the radius fiber is constant; hence the axisymmetric configuration should always be preferred, especially for the largest drops. However, we also notice in Fig. 1 different points. The larger the drop, the lower its center of mass, which stresses the increasing influence of gravity. The fiber is smaller than the capillary length $\kappa^{-1} = \sqrt{\gamma/\rho g}$ (denoting ρ and γ as the liquid density and surface tension; κ^{-1} is 1.5 mm for silicon oils), but the largest drops have a diameter of 1000 μm, which becomes of the order of κ^{-1}. Hence the observed shapes are barrel shapes deformed by gravity.

All the drops in Fig. 1 are at rest, which shows that gravity (for large drops) can be balanced by capillary forces (referred to as f_c). This equilibrium cannot hold for very large drops: a capillary force is bounded, while the drop weight increases as R^3 (with R the drop radius). We thus expect a threshold radius R_M above which a drop will detach. We note the corresponding threshold volume Ω_M (with $\Omega_M = 4\pi R_M^3/3$).

2.2. Critical size of hanging drops

We measured the volume Ω_M by increasing the volume of a drop by small increments of volume $\delta\Omega = 0.5$ mm^3 till the drop detached (Fig. 2 shows the dynamics of detachment for a drop just above the threshold). Ω_M is taken as the volume of the detaching drop, which yields an error of 0.05 mm^3 on its determination (the same experiment being performed several time approaching the critical volume).

We display in Fig. 3a the quantity R_M as a function of the fiber radius b. Both lengths are normalized by the capillary length κ^{-1}. The data are obtained with different liquids of various viscosities and surface tensions, which all wet the copper fiber completely. The typical error on these data is of order 15%.

In the linear presentation of the results (Fig. 3a), it is observed that all the data collapse onto the same curve. In particular, the liquid viscosity does not play any role, as expected in a static configuration. In the limit of large radius ($b > \kappa^{-1}$), R_M is found to tend toward a constant value, about 1.6 times the capillary length. For thin fibers ($b < \kappa^{-1}$), R_M increases rapidly with the radius of the fiber.

The same data can be plotted in logarithmic coordinates (Fig. 3b), which makes it possible to make the law precise for small radii. The data are well described by a scaling law of the type $(b\kappa)^\alpha$ over two decades, with a best fit value $\alpha = 0.33 \pm 0.10$ ($R_M = 1.53 b^{1/3}\kappa^{-2/3}$), in agreement with a scaling law first proposed by Hung and Yao [3]. We also observe in Fig. 3b that the transition between this regime and the saturation regime is located around $b\kappa = 1$.

3. Discussion

These results can be understood by considering the different characteristic lengths of the system. For a fiber radius larger than the capillary length, the curvature of the substrate

Fig. 1. Drops of silicon oil of various volumes ($\Omega = 0.01$, 0.10, 0.23, 0.32, and 0.52 mm^3, from left to right) hanging from a horizontal fiber of radius $b = 12$ μm.

Fig. 2. Set of pictures showing a drop of silicon oil falling off a fiber of radius $b = 350$ μm. The volume of the drop is just above Ω_M, so that gravity dominates the capillary force: the drop falls (interval between two successive pictures: 1 ms).

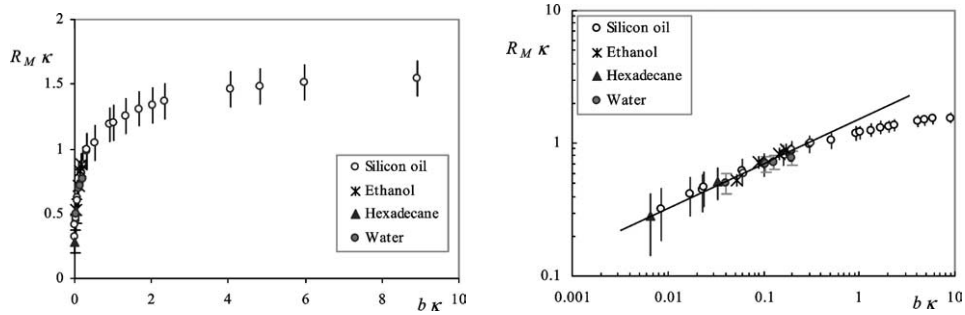

Fig. 3. Radius R_M of the largest drop hanging on a fiber, as a function of the fiber radius b. Both quantities are normalized by the capillary length κ^{-1} and are drawn in normal coordinates (a) or in logarithmic ones (b).

is very low, and the liquid behaves as if it were hanging from a flat solid surface (such as a ceiling). The maximal volume Ω_M of such a pendant drop must scale as κ^{-3}, since the capillary length is the only length in the system, as stressed by Boucher and Evans [9]. Moreover, Padday and Pitt [10] calculated this volume numerically and found Ω_M to be equal to $18.93\kappa^{-3}$, which thus yields $R_M = 1.65\kappa^{-1}$. This result is in very good agreement with our experimental observation since the saturation of R_M was found to be $1.6 \pm 0.1\kappa^{-1}$.

Things get more complicated for thin fibers ($b < \kappa^{-1}$). Dimensionally, this problem is very similar to the question of the maximal volume of a drop pending from a cylindrical nozzle of radius a. As shown by Tate [11], balancing the weight of the drop $4\pi\rho g R^3/3$ with the (maximum) force of surface tension $2\pi\gamma a$, we get $R_M = (3/2)^{1/3}a^{1/3}\kappa^{-2/3}$. Using dimensional analysis, Rayleigh [12] got the same result and proposed to introduce a dimensionless function f to describe the variation of the numerical coefficient: $R_M = f(\kappa a)(3/2)^{1/3}a^{1/3}\kappa^{-2/3}$. Harkins and Brown [13] studied this function experimentally (now referred to as the Harkins and Brown factor) and found that it remains in the interval [0.8, 1].

At a scaling level, Tate's law is in very good agreement with our experimental observations. The solution of both problems lies in a balance between gravity and capillary forces, of respective orders $\rho g R^3$ and γb. There is nevertheless a difference between the two numerical coefficients: while Tate's law predicts a coefficient between 0.91 and 1.14, we find 1.53 for this factor, in the experiment of drops on horizontal fibers. This implies that the maximum volume of hanging liquid is significantly larger if the fiber is horizontal than if it is vertical.

A way to model large drops hanging on thin fibers consists in making the assumption sketched in Fig. 4. We assume that the force resulting from the horizontal fiber is equivalent to the force generated by two similar fibers connected to the drop at the same location (characterized by the angle α), yet pointing radially.

Since the liquid wets the fiber, the capillary force acting along each fiber is simply written $2\pi b\gamma$, so that the total force pointing upward is $4\pi b\gamma\cos(\pi/2-\alpha)$. Balancing this

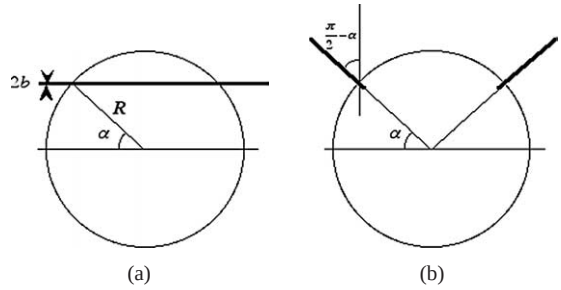

Fig. 4. (a) Sketch of a drop hanging from a fiber of radius b. (b) Configuration assumed as equivalent, with two fibers joining the drop at the same points as in (a).

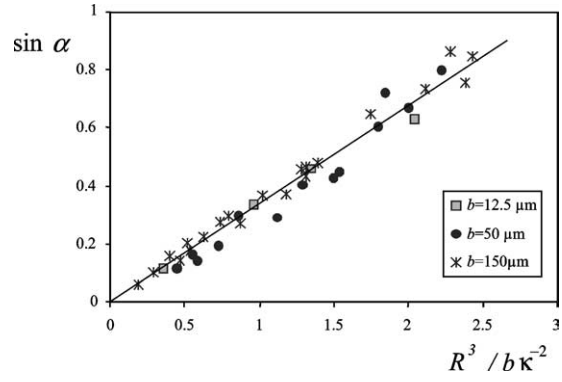

Fig. 5. Sine of the angle α (see Fig. 4 for the definition of α) as a function of $R^3/b\kappa^{-2}$, R being the drop size, b the fiber radius, and κ^{-1} the capillary length.

force by the weight yields an expression for the angle α:

$$\sin\alpha = \frac{1}{3}\frac{R^3}{b\kappa^{-2}}. \tag{1}$$

In the limit of small drops ($R \ll b^{1/3}\kappa^{-2/3}$), we find that α tends toward 0, which corresponds to the axisymmetric configuration (drops on the left, in Fig. 1). Equation (1) can be easily tested, by measuring the value of α, from pictures such as in Fig. 1: experiments were performed with three fiber radii and various drop volumes. The results are displayed in Fig. 5, where the sine of α is plotted as a function of the dimensionless quantity $R^3/b\kappa^{-2}$.

A linear relation is indeed found between these two quantities, and the numerical coefficient deduced from the data is 0.34 ± 0.03, in excellent agreement with the value (1/3) expected from Eq. (1).

Equation (1) no longer has solutions if the quantity $R^3/b\kappa^{-2}$ is larger than 3. Then the drop detaches, which yields as a maximum size for a drop hanging on a horizontal fiber:

$$R_M = 3^{1/3} b^{1/3} \kappa^{-2/3}. \quad (2)$$

This expression corresponds to the scaling observed experimentally in Fig. 3. In addition, the numerical coefficient (about 1.44) is close to the value deduced from Fig. 3 (1.53), although slightly smaller. The way we measure might explain part of this small discrepancy: volume is added till the drop detaches, which leads to a possible overestimate of the maximum volume of a hanging drop.

We can finally deduce from the above argument the maximum capillary force F_c acting on the drop, still in the limit $b \ll \kappa^{-1}$. It can be written

$$F_c = 4\pi\gamma b. \quad (3)$$

There again, this value is close (yet slightly smaller) to the measured maximum force (i.e., $4\pi/3\rho g R_M^3$), which is of the order of $15\gamma b$.

4. Dynamics

4.1. Observations

We now investigate the dynamics of the capture, and only consider drops smaller than R_M—since they are the only ones likely to be captured as hitting the fiber: a free-falling drop of radius R impacts a horizontal nylon fiber of radius b (80 µm $< b <$ 350 µm) at a velocity V, as sketched in Fig. 6. Drops of radius in the range between 0.5 and 1.5 mm ($R > b$) are dropped from a nozzle placed above the fiber, at a distance which can be varied conveniently between 0.5 and 10 cm, which yields 10 cm/s $< V <$ 100 cm/s. The whole device is adjusted in such a way that the center of mass of the drop falls on the fiber axis.

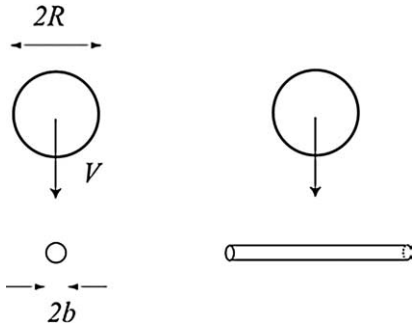

Fig. 6. Sketch of the experiment: a drop of radius R falls on a horizontal fiber of radius b.

Fig. 7 shows a sequence obtained with a drop of silicon oil (of viscosity $\eta = 5$ mPa s) impacting a horizontal fiber of radius $b = 350$ µm at a velocity of 20 cm/s. It is observed that in such conditions, the drop is entirely captured by the fiber.

When the same drop impacts the fiber at a higher velocity ($V = 95$ cm/s), most of the liquid is ejected from the fiber, and only a small fraction is captured by the fiber as can be observed in Fig. 8. The threshold velocity for liquid ejection is well defined and denoted furthermore as V^*. This threshold was determined, starting from a capture sequence, and increasing gradually the impact speed till part of the drop crosses the fiber. For each experiment, the velocity was measured using a high-speed video camera.

4.2. Critical velocity of capture

As emphasized in the previous section, capillary forces and gravity are antagonistic: the weight of the drop tends to detach it from the fiber, while surface tension is responsible for the sustentation. For analyzing the dynamics of the capture of a drop by a fiber, we must also consider viscous and inertia effects. Here again, those effects are antagonistic: while inertia tends to make the drop cross the fiber, viscous effects will induce a dissipation, and can thus possibly stop the drop. The different forces can be compared by using dimensionless numbers: in the limit considered here of low viscosity liquids, the Reynolds number based on the size of the fiber is large and the drag scales as $\rho V^2 bR$. The Weber number (denoted furthermore as $We = \rho V^2 R/\gamma$) thus evaluates the relative importance of the two sticking forces, whereas the Froude number $Fr = V^2/2gR$ compares the forces allowing the crossing (i.e., inertia and gravity). For a drop of water ($\eta = 1$ mPa s) of radius $R = 1$ mm falling on a fiber of radius $b = 150$ µm, we measure 40 cm/s for the critical velocity of crossing. The corresponding Reynolds number is 60 and the Weber number is 2.3 indicating that the drag is of the same order as the capillary force. On the other hand, Fr is found to be in this example of the order of 1 (Fr = 7), which shows that both inertia and gravity should be taken into account.

In the complementary situation where a drop impacts a surface pierced with a hole, the critical velocity for crossing the hole was found to be independent of the size of the drop [5]. This is obviously untrue here: we already understood in Section 2 that drops of radius larger than R_M could not stand at rest on the fibers. Hence we can only define a velocity of crossing for drops smaller than R_M. We report in Fig. 9 the critical velocity of crossing, V^*, as a function of the radius of the impacting drop for different fiber radii.

We observe that the crossing velocity decreases with increasing drop radius, which seems quite obvious: large drops are less likely to be captured than small ones. This behavior becomes critical as R approaches R_M (i.e., as V^* tends to zero). Moreover, for a given drop, the thicker the fiber, the higher the velocity of crossing, in agreement with the results

Fig. 7. Set of pictures taken each 4 ms (front view, as sketched in Fig. 6a). The drop of silicon oil ($\eta = 5$ m/s) falling at 20 cm/s is entirely captured by the fiber.

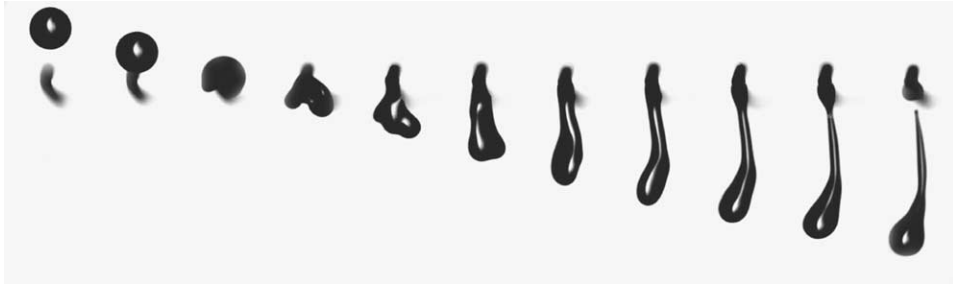

Fig. 8. A drop of silicon oil ($\eta = 5$ mPa s) impacting at $V = 95$ cm/s a horizontal fiber of radius $b = 350$ μm is not trapped by the solid. An elongated drop forms below the fiber and eventually detaches, and only a small amount of liquid remains captured. Interval between successive pictures 2 ms.

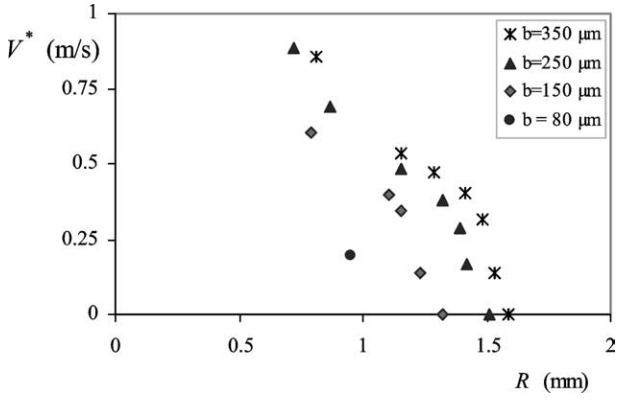

Fig. 9. Critical velocity for crossing a fiber of radius b, as a function of the radius of the impacting drop R. The drops consist of water, and the fibers of nylon.

of Section 2, where it was shown that the capillary force increases (linearly) with the fiber radius. In the next section, we will interpret quantitatively these results.

5. Discussion

For low-viscosity liquids, the Reynolds number based on the size of the fiber is large and the force exerted by the fiber on the drop is $F_D = 4C_D\rho V^2 Rb$, where C_D is the drag coefficient, of order unity for cylinders. Taking $F_C = 4\pi b\gamma$ for the capillary force, the evolution of the velocity of the drop of mass M is described by Newton's law:

$$M\frac{dV}{dt} = -F_D - F_C + Mg. \tag{4}$$

We denote x as the axis pointing downward and having its origin at the position of the center of gravity of the drop when it contacts the fiber (Fig. 10). With $V_M = \sqrt{4gR_M}$ and

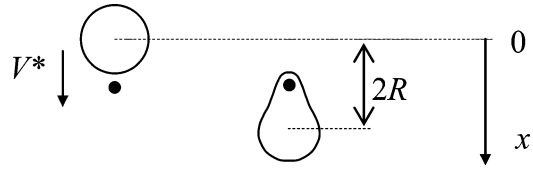

Fig. 10. Position of the drop before and after the impact on the horizontal fiber.

R_M as the characteristic velocity and length, the nondimensional form of Eq. (4) is

$$\frac{d\overline{V}^2}{d\bar{x}} + \frac{6C_D}{\pi}\frac{b}{R}\overline{V}^2 = -\frac{1}{2}\left[\left(\frac{R_M}{R}\right)^2 - \frac{R}{R_M}\right], \tag{5}$$

where the reduced quantities are overlined. This equation must be integrated with the initial condition $\overline{V}(\bar{x} = 0) = \overline{V_0}$. The solution of this system describes the evolution of the velocity with the penetrating distance $\bar{x}$,

$$\overline{V}^2 = \overline{V_0}^2 e^{-(kR_M/2R)\bar{x}} - \frac{R}{kR_M}\left[\left(\frac{R_M}{R}\right)^2 - \frac{R}{R_M}\right]\left[1 - e^{-(kR_M/2R)\bar{x}}\right], \tag{6}$$

where $k \equiv 12C_D b/(\pi R_M)$ is a constant for a given fiber and liquid. The condition for the capture is $\overline{V}(\bar{x} = 2) = 0$. According to Eq. (6), this condition is satisfied for the impact velocity:

$$\overline{V^*}^2 = \frac{e^{kR_M/R-1}}{kR_M/R}\left[\left(\frac{R_M}{R}\right)^2 - \frac{R}{R_M}\right]. \tag{7}$$

This critical velocity of capture (naturally) vanishes for $R = R_M$. In the limit $k \ll 1$, it reduces to

$$V^* \approx V_M\left[\left(\frac{R_M}{R}\right)^2 - \frac{R}{R_M}\right]^{1/2}. \tag{8}$$

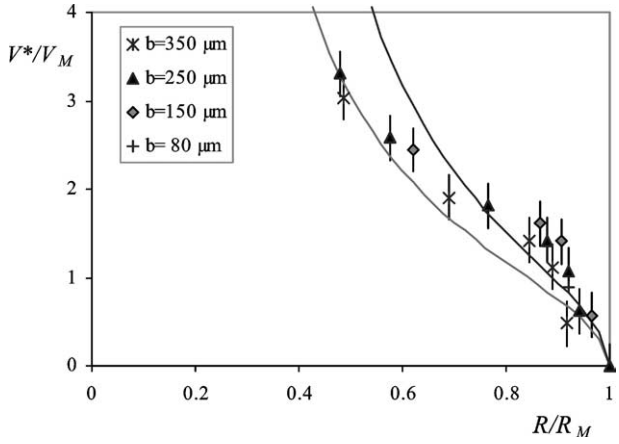

Fig. 11. V^*/V_M as a function of R/R_M for different fiber radii; R_M and V_M are defined in Eqs. (2) and (5). The experimental data collapse onto the same curve, which is quite well fitted by Eq. (7), drawn in full line for two fiber radii ($b = 150$ µm, in gray, and $b = 350$ µm, in black).

In this very thin fiber limit, the critical velocity is only a function of the ratio R/R_M, and indeed qualitatively exhibits the main features observed in Fig. 9: V^* decreases as $1/R$ for small R, and vanishes as $\sqrt{R_M - R}$ when R tends toward R_M.

As suggested by this discussion, the experimental results of Fig. 9 are replotted in Fig. 11 in dimensionless form. We first observe that with this rescaling, all the measurements collapse on the same curve. The analytical evaluation of the critical velocity given by Eq. (7) is also presented with a solid line in Fig. 11, for two different fibers (on the left $b = 150$ µm, and on the right $b = 350$ µm) and using $C_D = 2$ and $V_M = 1.1\sqrt{4gR_M}$. It is observed that the theoretical curves slightly change when modifying the fiber radius, but the general trends remain the same and capture quite well the experimental observations.

6. Conclusion

We studied the statics and the dynamics of a drop falling on a horizontal fiber. For the static, we characterized the position of a drop on a fiber as a function of its size and studied the radius of the largest drop that can remain stuck. This radius was found to scale as the radius of the largest drop that can hang from a vertical needle, which was explained using dimensionless arguments. Nevertheless we stressed on the difference of the prefactor: a horizontal fiber is able to hold a drop about two times heavier than a vertical nozzle of same radius.

This critical radius defines the size of the largest drop that can be totally captured by a fiber which it impacts. We showed that for drops smaller than this critical size, different situations can occur. Above a threshold velocity, most of the liquid is ejected from the fiber, while below this threshold the drop is entirely captured by the fiber. For liquids of low viscosity, the threshold was shown to be set by a balance between inertia, the drag of the fiber, gravity and capillary forces. The study of this threshold velocity in the viscous limit remains to be done.

Acknowledgment

We sincerely thank an anonymous referee for very valuable comments and suggestions.

References

[1] P. Contal, J. Simao, D. Thomas, T. Frising, S. Calle, J.C. Appert-Collin, D. Bemer, J. Aerosol Sci. 35 (2004) 263.
[2] P. Patel, E. Shaqfeh, J.E. Butler, V. Cristini, J. Blawzdziewicz, M. Loewenberg, Phys. Fluids 15 (2003) 1146.
[3] L.S. Hung, S.C. Yao, Int. J. Multiphase Flow 25 (1999) 1545.
[4] A. Rozhkov, B. Prunet-Foch, M. Vignes-Adler, Phys. Fluids 14 (2002) 3485.
[5] E. Lorenceau, D. Quéré, J. Colloid Interface Sci. 263 (2003) 244.
[6] B.J. Carroll, J. Colloid Interface Sci. 97 (1984) 195.
[7] G. McHale, N.A. Käb, M.I. Newton, S.M. Rowan, J. Colloid Interface Sci. 186 (1997) 453.
[8] G. McHale, M.I. Newton, Colloids Surf. A 206 (2002) 79.
[9] E.A. Boucher, M.J.B. Evans, Proc. R. Soc. London Ser. A 346 (1975) 349.
[10] J.F. Padday, A.R. Pitt, Philos. Trans. R. Soc. London 275 (1973) 489.
[11] T. Tate, Philos. Mag. 27 (1864) 176.
[12] Lord Rayleigh, Philos. Mag. 48 (1899) 321.
[13] W.D. Harkins, F.E. Brown, J. Am. Chem. Soc. 41 (1919) 499.